Global Medical and Health Communication

Online submission: https://ejournal.unisba.ac.id/index.php/gmhc
DOI: https://doi.org/10.29313/gmhc.v12i3.13386

GMHC. 2024;12(3):169–179
pISSN 2301-9123 | eISSN 2460-5441

RESEARCH ARTICLE

Promotion of Crypt-like Structures in Intestinal Organoid Development through the Addition of Graphene Oxide in Cell-based Assays

Haura Labibah Salsabil Sulaksono,[1] Mutiara Mila Kamilah,[2] Lia Faridah,[2,3] I Made Joni,[4,5] Kozo Watanabe,[6] Savira Ekawardhani[2,3]

[1]Master of Biotechnology Study Program, Graduate School Universitas Padjadjaran, Bandung, Indonesia, [2]Parasitology Laboratory of Human, Safety, and Environment (HSE), Universitas Padjadjaran, Bandung, Indonesia, [3]Department of Biomedical Sciences, Faculty of Medicine, Universitas Padjadjaran, Bandung, Indonesia, [4]Functional Nano Powder University Center of Excellence (FiNder U-CoE), Universitas Padjadjaran, Bandung, Indonesia, [5]Department of Physics, Faculty of Mathematics and Natural Science, Universitas Padjadjaran, Bandung, Indonesia, [6]Department of Civil and Environmental Engineering, Ehime University, Matsuyama, Japan

Abstract

The intestinal organoid represents a miniature organ that can mimic functional physiology and pathology. However, there are several challenges to developing the organoid system, such as the limited survival of cells. Based on theory, matrix addition is a factor that can support survival in cells. As a result, graphene oxide (GO) addition is used in this study. As an artificial matrix, GO has been successfully shown to encourage good cell behavior and is well known for having good biocompatibility. Herein, we fabricate GO characterized with FT-IR and PSA. Crypt-like structures (CLS) are isolated from small intestinal mice in GO addition as a matrix. The gene expression and cell viability of CLS are investigated. RT-PCR examined the gene expression in CLS, while cell viability of CLS was carried out using the staining method. This study was conducted at FiNder U-CoE and Parasitology Laboratory of HSE Universitas Padjadjaran Bandung during February and December 2023. Our results show that Vil-1 as an identity for cells in the intestinal epithelium has been expressed in CLS primary significantly higher than intestinal tissue (p=0.01). However, identifying Lgr5 in CSL isolates is tricky. Thes in the crypt may be limited. Besides that, cell viability of CLS with GO addition can be maintained for four days. The GO addition as a matrix may provide support to maintain CLS. These findings are promising as cell-based assays for developing organoid models.

Keywords: ElimCell culture, graphene oxide, matrix, organoid

Introduction

Cell-based assays have been an important component of drug discovery because they provide a simple, quick, and cost-effective technique for avoiding large-scale and costly animal testing.[1] Two-dimensional (2D) cell cultures as traditional in vitro assays have been widely used in the pharmaceutical industry for drug discovery.[2] However, these assays have several obstacles, such as not being able to control cell shape, losing the ability to regulate cells, being limited to a single type of cell, and not being able to reflect the physiological complexity of the tissue so that it can produce bias in predicting specific tissue responses.[1,3] Recently, three-dimensional (3D) cell cultures have been developed as a better model for evaluating and promoting improved cell- and organ-based assays for representative physiology and better drug response prediction.[4,5] The intestinal organoid is one of the most commonly used models. Previous studies have shown that the intestinal organoid can recapitulate functional physiology and pathology.[6,7] Furthermore, the intestinal organoid has shown successful models that may simulate the native organ, including gene and protein expression, metabolic activity, tissue engineering, and even pathology, which is greater than 2D cell culture models.[8,9] However, there are obstacles to creating the organoid system, such as constraints in culture system survival and maturity, even cell function, and a high level of cell variability.[9] Furthermore, studies with references showed the

Received: 13 January 2024; Revised: 18 July 2024; Accepted: 24 July 2024; Published: 16 December 2024

Correspondence: Savira Ekawardhani. Department of Biomedical Sciences, Faculty of Medicine, Universitas Padjadajaran. Jln. Prof. Eyckman No. 38, Bandung 40161, West Java, Indonesia. E-mail: savira@unpad.ac.id

limitations of survival in the culture system for developing intestinal organoid models.[7,10]

Matrix addition is one of the factors that influences organoid culture outcomes.11 Moreover, matrix addition is a significant factor in developing organoids to decrease cell apoptosis by maintaining survival in the culture system.[12] Culture organoids are grown in matrigel as a matrix.[13,14] However, xenogenic contaminants are found in matrigel, and variability in the composition of matrigel makes the development of organoids challenging.[15,16] Xenogenic contaminants detected in matrigel can interfere with organoid behavior.[16] Furthermore, heterogeneity in the composition of matrigel encourages variability in the physical and biochemical properties of matrigel, which makes it difficult to manipulate cell behavior and obtain precise biological responses.[16] Interestingly, graphene oxide (GO), a synthetic material, has been employed as an artificial matrix in tissue engineering and regeneration, displaying its capacity to direct cell behavior effectively.[17,18] GO can increase mechanical characteristics, promote cell proliferation and adhesion, have a high water absorption capacity, have no effect on cytotoxicity, and even have antioxidant capabilities to neutralize free radicals because GO possesses electrons on its surface.[19] GO has also been demonstrated to regulate gene expression in tissue engineering and regeneration.[20,21] Therefore, GO may have the potential for developing organoid models because it encourages good behavior by creating a microenvironment in vivo.[20,22]

This study aimed to investigate the effects of GO addition as supported factors such as CLS culturing. Maintaining CLS's structures and cell viability in the addition matrix is the first step in developing an intestinal organoid model as a cell-based assay.

Methods

This study was carried out between February and December 2023 at the Parasitology Laboratory of HSE and FiNder U-CoE Universitas Padjadjaran Bandung. Materials used in this study: phosphate buffered saline/PBS (Sisco Research Laboratories), trypsin/EDTA 0.25% (PAN-Biotech), fetal bovine serum (Sigma-Aldrich), penicillin-streptomycin (PAN-Biotech), gentamicin (PAN-Biotech), Dulbecco's modified eagle medium/DMEM (PAN-Biotech), insulin human recombinant (PAN-Biotech), hydrochloric acid fuming 37% (Supelco), ethanol, graphite (Merck), HCl (Supelco), $NaNO_3$ (Merck), $KMnO_4$, H_2SO_4, H_2O_2 (Merck), distilled water, silicon oil, ice, NaCl, propidium iodide (Sigma-Aldrich).

GO synthesis is carried out by a modified method based on protocol with references.[23] Graphite (4 g) and 2 g $NaNO_3$ were put into the tube and stirred until mixing. After that, pour H_2SO_4 slowly. In the ice bath phase, the tube was placed in a container filled with ice, and the mixture was stirred for 30 minutes. 10 g $KMnO_4$ was added slowly and stirred for 30 minutes. The ice is discarded in the container while the tube remains above the stirrer. The container was filled with silicone oil, and the tube was placed in the container. Increase the temperature by 35–40°C by maintaining the temperatures at 35°C and stirring for 1 hour (at this point, the color typically changes to brown). Then, 90 ml of distilled water was slowly added, and the temperature was raised to 98°C and stirred for 40 minutes (at this point, it usually turned a brownish color that became increasingly clear). Distilled water (400 ml) was added to the mixture, and then 50 ml of H_2O_2 was slowly added and stirred for 30 min. Subsequently, the mixture was left overnight.

The following day, after it settles, the clear liquid part is discarded while the settled part is retained. Then, 10 ml of HCl was added, stirred for one hour, and allowed to settle. After it settles, take a temperature measurement and discard the top part of the clear liquid, maintaining the part that has settled. Then, 2,500 ml of distilled water was added, stirred for 30 min, and left to settle (centrifugation stage and repeated pH measurements). Centrifugation (at 10,000 rpm for 5 minutes) was repeated to separate the settled and transparent liquid. In contrast, temperature measurements were carried out to obtain a neutral pH according to the pH of the distilled water used. After the pH reached neutral, it was dried at 60°C.

Structures were characterized using FT-IR (Thermo Scientific Nicolet iS5 in the wavenumber range of 400–4,000 cm^{-1}) and particle measurement using particle size analysis/PSA (Horiba Scientific SZ-100).

Ethical approval was obtained from the Research Ethics Committee at the University of

Padjadjaran, 576/UN6.KEP/EC/2023. Male mice of Wistar swabs of 6–12 weeks-old swabs were obtained from the Animal Laboratories Eijkman, Faculty of Medicine, Universitas Padjadjaran. In the present study, the mice were sacrificed by the physical cervical dislocation method.

The CLS–isolation method is modified based on protocol with references.[24,25] A mouse was sacrificed according to ethical approval regulations, dissected, and harvested 15 cm of the small intestine proximal to the stomach. The segment was then placed into a Falcon tube (50 ml) with 15 ml cold PBS (2–8°C) and gentamicin 0.5 mg/ml. Shake the Falcon tube in the circle for 5 minutes to remove contaminants attached to the intestinal segment. Next, tweezers transfer the intestinal segment to a dish containing 10 ml of cold PBS (2–8°C). The intestinal segment was cut lengthwise using scissors and rinsed to remove fat attached to the tissue. Transfer the intestinal segment to a new dish containing cold PBS (2–8°C) and rinse (repeat steps two times, ensure the fatty tissue and contaminants are removed). Cut the intestinal segment into 4–8 mm pieces and place into 50 ml of the Falcon tube with 15 ml cold PBS containing gentamicin (0.5 mg/ml) and vortex at 250 rpm for 5 minutes to remove contaminants. Discard the supernatant, add 15 ml of cold PBS (2–8°C) to a 50 ml Falcon tube, and shake 15–20 times in a circular motion (repeat these steps three times).

After that, add 15 ml of cold PBS (2–8°C) to a 50 ml Falcon tube and use a serological pipette to pipette the intestinal pieces up and down five times gently. After that, shake it 15–20 times in a circular motion, then remove the supernatant (repeat this step 15–20 times or until the supernatant is clear). When the supernatant is clear, remove it and resuspend the tissue pieces in 10 ml of cell dissociation reagent at room temperature (15–25°C) and incubate it for 10 minutes while shaking slowly in a circular motion and allowing the tissue pieces to settle by gravity. Pipette off and discard the supernatant, leaving just enough liquid to cover the tissue pieces. Resuspend the tissue pieces in 10 ml cold PBS (2–8°C) containing 0.1% FBS (2–8°C) and vortex at 250 rpm for 20 seconds, allowing the tissue pieces to settle in the below. Transfer the supernatant carefully with a pipette and filter it through a 70 μm filter.

Then, collect the filtrate in a new 50 ml Falcon tube. Discard the filter, label the filtrate "Fraction 1," and place the fraction on ice. Following that, resuspend the tissue pieces in 10 mL of cold PBS (2–8°C) containing 0.1% FBS (2–8°C) and vortex at 250 rpm for 20 seconds, allowing the tissue pieces to settle in the below (repeat these steps to get Fraction 2–4). After getting four fractions, centrifuge each fraction at 290 RCF for 5 minutes. Pipette off and discard the supernatant, retaining the pellet in each tube. Resuspend each pellet in 10 ml of cold PBS (20–8°C) containing 0.1% FBS (2–8°C), then centrifuge at 200 RCF for 3 minutes. Carefully discard the supernatant, retaining the pellet in each tube.

After obtaining four fractions, resuspend each fraction in 4 ml of cold DMEM/F12 (2–8°C) to prevent and reduce cell damage. Add 1 ml of each fraction using an inverted microscope. Select two fractions enriched with intestinal CLS (CLS that are desirable for culture can be of various sizes, typically rectangular or singular in shape; usually, fractions 3 and 4 are enriched CLS). Mix fractions 3 and 4 and transfer 1 ml to the labeled two Falcon tubes of 15 ml (the number of Falcon tubes is adjusted to the number of treatments; CLS without GO and CLS with GO, then centrifuge each Falcon tube at 200 RCF for 5 minutes and discard the supernatant, retaining the pellet in the bottom of each tube. Next, add 150 μl of the CLS medium at room temperature (15–25°C) to each tube, then add 150 μl of treatment as a matrix (GO) to the labeled Falcon tube. Carefully pipette 50 μl of each suspension into the center of each of the six wells of the pre-warmed 24-well plate. Place the plate at 37°C for 10 minutes, then add 750 μl of medium crypt complete at room temperature (15–25°C) by carefully pipetting the medium down the side wall of each well. Transfer and place the lid on the culture plate, then incubate at 37°C and 5% CO2. Finally, it was observed using an inverted microscope regularly and changed with 750 μl of fresh medium complete at room temperature (15–25°C) three times for a week.

RNA isolation was prepared by harvesting the CLS from each well of the plate with 150 μl cell dissociation reagent in each well of the plate. Then, they are transferred to the labeled Falcon tube of 15 ml containing 1 ml DMEM (the labeled Falcon tube is adjusted for each treatment). Centrifuge at 290 RCF for 3 minutes, discard the supernatant, and retain the pellet. Add 150

Table 1 Quantitative RT-PCR Primers

Primer	Gene for Mouse	Forward Primer	Reverse Primer
Lgr5	Stem cells intestinal	GACGCTGGGTTATTTCAAGT TCAA	CAGCCAGCTACCAAATAGGT GCTC
Vil-1	Enterocytes	GACGTTTTCACTGCCAATACCA	CCCAAGGCCCTAGTGAAGTCTT
GAPDH	Housekeeping gene	AACTTTGGCATTGTG GAAGG	ACACATTGGGGGTAG GAACA

µl of DMEM to each pellet and then transfer to a microtube. After obtaining CLS, RNA isolation from CLS is received by an RNA extraction kit (MagEX). Besides that, real-time PCR preparation uses mixing PCR (SensiFAST SYBR No-ROX One-Step Kit) and mixing each reagent according to kit composition to each labeled primer microtube. Quantitative RT-PCR was performed with a LightCycler®480 using SYBR Green I/HRM dye (465–510). The sequences of the PCR primer are listed in Table 1.[26] The experiments were carried out in triplicate.

Morphology CLS analysis was examined using a microscope (Inverted Biological Microscope, Labtron Equipment Ltd, UK). The gene expression of CLS measurement was carried out to identify cells of the epithelium intestinal.[26] Propidium iodide (PI) staining to show cell viability of CLS through CLS was seeded onto a 96-well plate and incubated for four days. To investigate the viability of CLS for four days, CLS without and with GO were treated with and without 5FU for four days and stained with PI.

Statistical significance was performed using Prism 9 (Grapadh Software, La Jolla, CA, USA). The number of CLS, death cells, and PCR data was analyzed with a t-test. Each experiment was repeated three times. Statistical significance was assumed for p-values<0.05.

Results

This study shows GO characterization, such as FT-IR and PSA. The varying presence of oxygen functional groups is measured with each wave peak consisting of 3,499 for the O-H group; 1,712 for the C=O group; 1,613 for the C=C group; 1,370 for the C-OH group; and 1,041 for the C-O group as shown in Figure 1A. Besides that, the PSA characterization of GO shows that GO is smaller after 30 minutes of sonication than before sonication, as shown in Figure 1B. The average size distribution of GO after sonication shows 84.5 nm (Figure 1B 2) compared to GO before sonication (Figure 1B 1), namely 697.8 nm. These results indicate that GO is dispersed by the

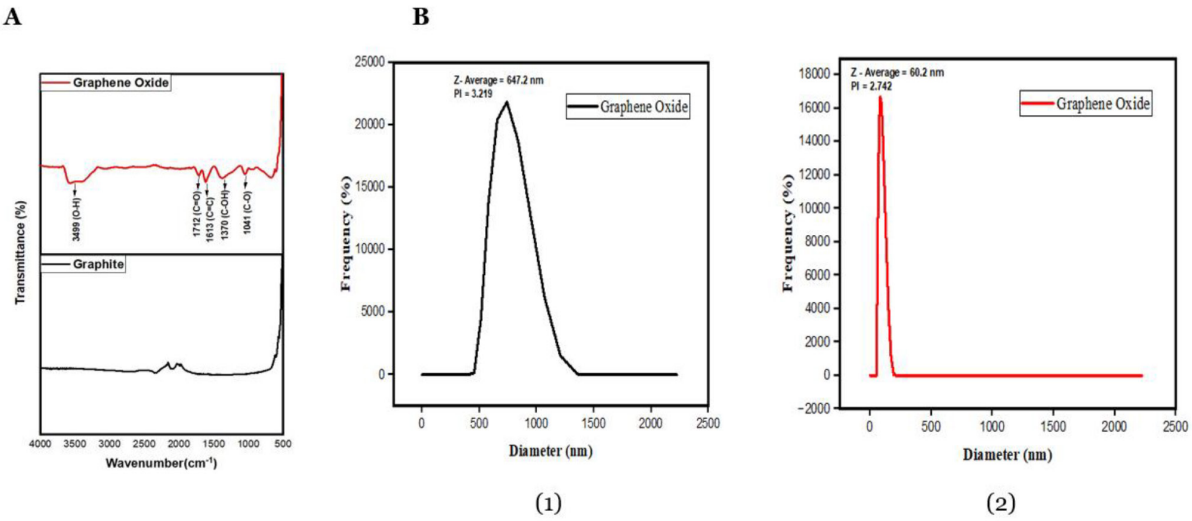

Figure 1 Graphene Oxide Characterization
Note: (A) FT-IR for graphite and GO; (B) the PSA analysis of GO before (1) and after (2) sonication

sonication waves, resulting in a smaller particle size.

The CLS isolation has been conducted successfully with enriched CLS as multicellular structures, as indicated by the circular mark for each CLS, as shown in Figure 2A. However, based on this observation, CLS is more enriched in fraction three than in fraction 4. Furthermore, fractions are conducted as CLS, identifying gene expression in the intestinal epithelium. Figure 2E shows the expression of Vil-1 is 1.1 fold and 0.14 fold for CLS primary and intestinal tissue, respectively. Furthermore, the expression Vil-1 in CLS primary was significantly higher than in intestinal tissue (p=0.0333; see Table 2).

Moreover, we seeded CLS without and with GO for five days, as shown in Figure 2B. Based on these results, GO addition can maintain CLS better than without GO addition during incubation time. Furthermore, Figure 2C shows the average number of CLS is 0 and 2.7 for CLS without GO and CLS with GO, respectively. However, the number of CLS without GO is 0 because it is contaminated by yeast (Figure 2B). Besides that, to investigate the effect of GO on maintaining CLS, we seeded CLS without and with GO for seven days (Figure 2C). Figure 2E shows the average number of CLS, which is 3.5 and 14 for CLS without GO and CLS with GO, respectively. In addition, there were no significant differences between the CLS without GO and those with GO (see Table 2). However, CLS GO addition can be maintained as the number of CLS with GO is higher than without GO, as shown in Figure 2E.

Fluorescence staining analyses were performed to investigate whether the viability of CLS can be maintained, which was triggered by 5FU-induced senescence. Figure 3A shows that the group with 5FU treatment demonstrated an alteration in their morphology that became larger and appeared like a dark spot, considered senescence-associated secretory (SASP). In addition, based on this observation, the viability of CLS can be maintained for 96 hours, even after it is treated with 5FU (Figure 3B). Furthermore, Figure 3C shows the average number of cell death is 93 for CLS without 5FU and 230.5 for CLS with 5FU. Based on these results, there were no significant differences among them (see Table 2). However, CLS can be maintained as the number of CLS without 5FU is lower than CLS with 5FU, as shown in Figure 3C.

Discussion

This study showed that GO has been synthesized successfully. The results of this FT-IR analysis indicate the presence of oxygen functional groups, such as hydroxyl (O-H), epoxy (C-O), carboxyl (C-OH), and carbonyl (C=O) of GO structures.[27] This result supported previous studies.[28,29]

Table 2 Statistical Analysis with the t-test

t-test Unpaired: Expression of Vil-1	**Sig.**	**t**	**df**	**F**	**Mean**	**95% CI**
Intestinal tissue	0.0333*	3.187	4	37.05	0.1449	0.1234 to 1.790
CLS primary					1.102	
Difference between ±SEM					0.9569±0.3002	
t-test Paired	**Sig.**	**t**	**df**	**SD of Difference**	**Mean of Difference**	**95% CI**
CLS with and without GO for five days	0.1567	2.219	2	2.082	2.667	−2.504 to 7.838
CLS with and without GO for seven days	0.0903	7.000	1	2.121	10.50	−8.559 to 29.56
CLS+GO with and without 5FU for cell viability	0.2754	2.165	1	89.90	137.5	−669.3 to 944.3

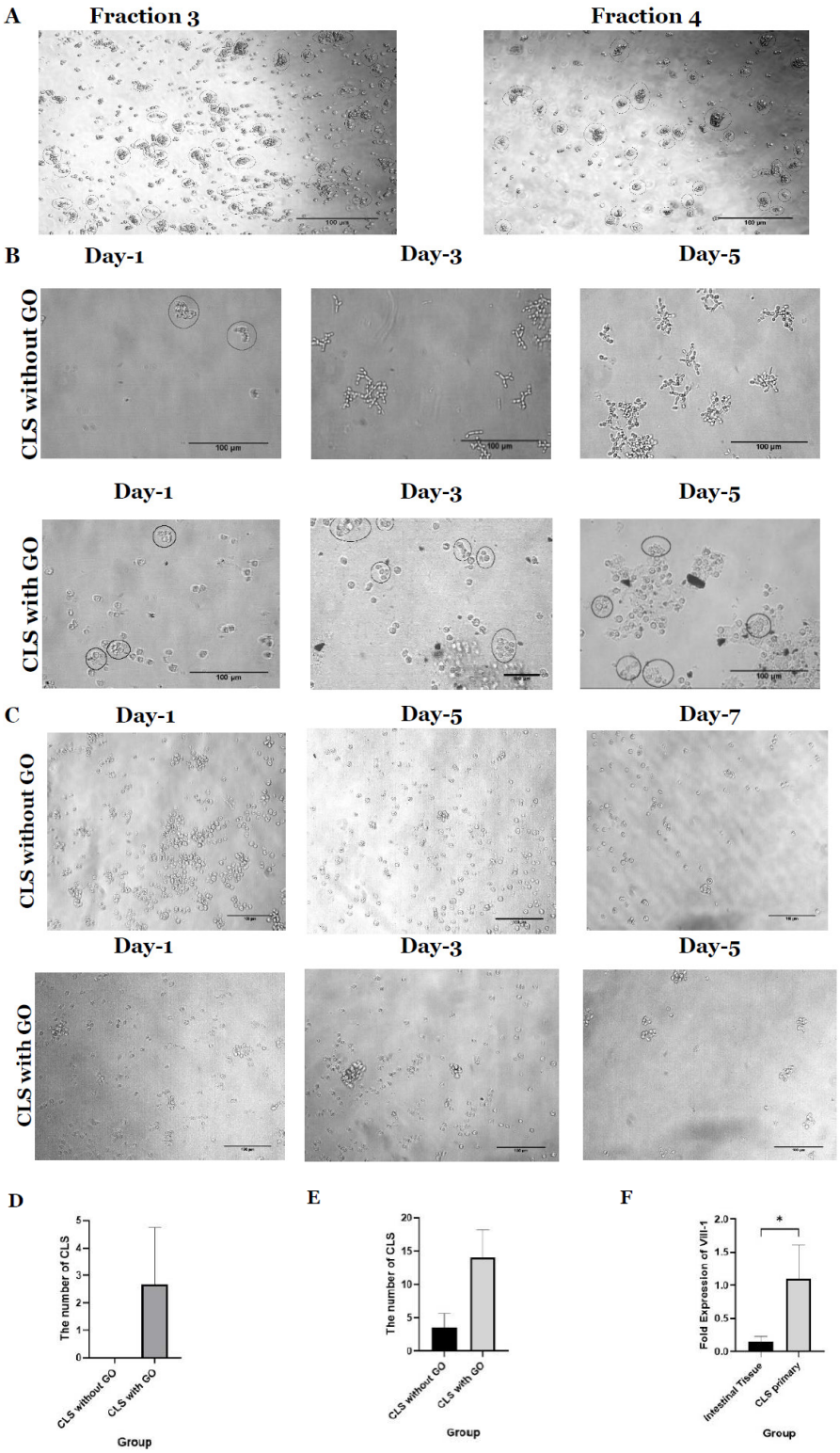

Figure 2 Crypt-like Structures Characterization

Note: (A) raw CLS were isolated, scale bar 100 µm with 10× magnification from the small intestines of Wistar swiped mice at 6–12 weeks; (B) CLS is seeded without and with GO for 5 days with 40× magnification, scale bar 100 µm; (C) CLS is seeded without and with GO for 7 days with 20× magnification, scale bar 100 µm; (D) the number of CLS without and with GO was quantified for 5 days; (E) the number of CLS without and with GO was quantified for 7 days; and (F) fold expression of Vil-1 as identified cells in epithelium intestinal with statistical significance considered *p<0.05 (n=2, t-test)

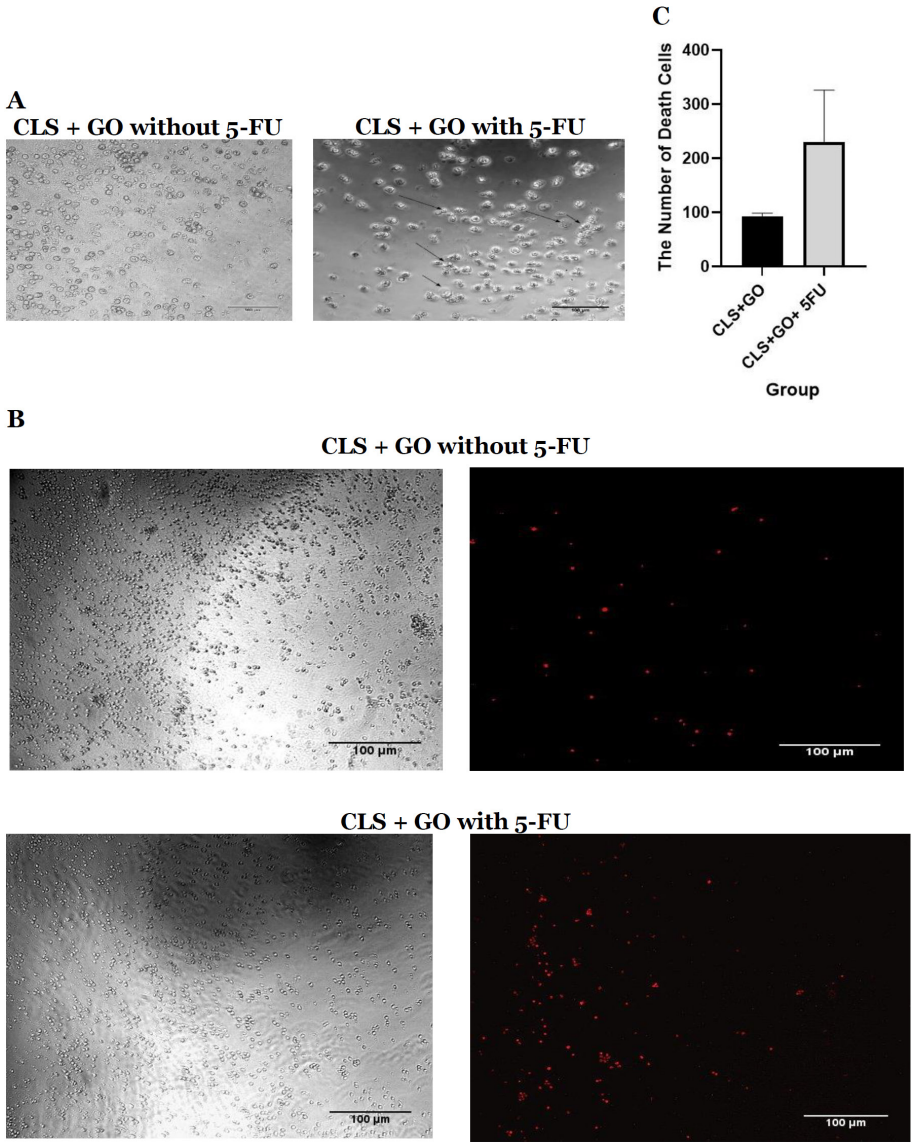

Figure 3 Cell Viability of CLS

Note: (A) morphology of CLS+GO without and with 5FU treatment with 20× magnification, scale bar 100 µm; (B) CLS+GO without and with 5FU treatment, before and after PI staining, respectively, with 10× magnification, scale bar 100 µm; and (C) the quantified number of death cells for 4 days

Furthermore, GO, which has been synthesized, was used in this study as a matrix addition for seed CLS isolation. In the present study, CLS isolation morphology has characteristics similar to previous studies.[30,31] These results indicated that CLS isolates have been successfully obtained. Besides that, we received 24 CLS (data not shown). Every crypt contains around 16 cells and around 20–25 cells in the lower and upper columns of the crypt, respectively. Furthermore, the crypt contains around 4–16 stem cells and 4–6 transit-amplifying cells (TA).[32] Crypt obtained from intestinal primary mice can be used for the development of organoids as organ miniatures that represent physiology and pathophysiology response.[33]

Various types of cells differentiate in the intestinal epithelium, such as enterocytes, goblet cells, path cells, and enteroendocrine cells originating from the Lgr5 cell stem found at the base of the intestinal crypt.[34] In this study, CLS isolates are examined for gene expression with genes of interest, such as Lgr5 and Vil-1, as a gene code in stem cells and enterocytes, respectively,

besides Gapdh being used as a housekeeping gene.[26] The housekeeping gene is a gene that is stably expressed in all cells of an organism, regardless of tissue type, developmental stage, and cell cycle state.[35] Gapdh is an internal gene commonly used in studies with gene expression.[36] Previous studies showed that Gapdh is a stable gene used as an internal control in studies using various cells and even for organoid model applications.[37,38]

The present study showed that CSL isolation is difficult to characterize for Lgr5. These results, supported by previous studies, showed that isolating and characterizing primary Lgr5 cells makes obtaining vibrant cultures in epithelial stem cells difficult.[39] It could be because the number of stem cells in the crypt is limited. Each of the crypts comprises approximately 15 stem cells in the mouse.[40] Furthermore, all stem cells compete for niche space between Paneth cells, which provide essential Notch ligands that can only be induced via direct cell-cell contact, so the present cell in a high-WNT environment is the limiting resource in the stem cell zone.[40,41] However, Lgr5 is one of the best characterized of these markers.[42]

Besides that, Vil-1 is used to identify cells in the intestinal epithelium. Vil-1 is a marker that codes enterocytes, the most common cells of the intestinal epithelium, even though it is found along the crypt-villus axis.[40] Furthermore, the small intestine can be identified by the presence of villi, whereas villi don't exist in the caecum and colon.[43] This study showed that fold gene expression of Vil-1 for CLS primary is higher than in intestinal tissue. These results supported the idea that Vil-1 as a marker is used to identify types of cells in the intestinal epithelium.

Besides that, CLS is seeded with GO, which has the highest average number of CLS without GO. These results suggest GO optimization may influence the maintenance of cell complex structures. These results supported that GO addition has effects on cell growth.[18] Besides that, GO-enhanced cell differentiation is required to generate multicellular cells.[17,21,44] Moreover, study with references showed that GO promoted good cell behavior, such as mimicking cell characteristics appropriated to the native cells,[17,20–22] improving proliferation,[18,22] and even regulating gene expression.[18,20–22] Furthermore, due to GO's morphology, shape, size, and even functional groups, it has unique structures and even improves cell interactions.[45] Therefore, in this study, we used the size of GO to be 84.5 nm. Moreover, GO with particle sizes below 100 nm shows no cytotoxic effects.[46]

In addition, CLS is seeded without GO, which is contaminated after the second day of incubation. It may be caused by the lack of control over the environment when the mice were sacrificed. Interestingly, CLS seeded in GO addition demonstrated no contamination. GO has unique physics characteristics, so it is antibacterial.[22] GO has oxygen groups that play significant roles for inactivated bacteria in cells through ROS activation, which induces oxidative stress and encourages an apoptotic pathway.[47] Moreover, a study with references showed that GO has antimicrobial effects, such as antibacterial, anti-fungal, and anti-yeast.48 GO has unique structures, so it has hydrophilic properties that are preferred in cells because it prevents cell agglomeration, impacts nutrient limitation, and even induces oxidative stress, which promotes cell apoptosis.[49] Therefore, GO optimization can maintain the cell viability of CLS. Furthermore, this study showed that the number of death cells in CLS+GO without 5FU was lower than in CLS+GO with 5FU for four days. It indicated that the cell viability of CLS can be maintained.

Conclusions

In the present study, we found that Vil-1, which is identified as a cell in the intestinal epithelium, is expressed in CLS primary successfully. CLS is seeded with GO addition, which can help maintain multicellular structures. Furthermore, the viability of CLS has shown that it can be maintained. To conclude, this finding supports cell-based assays, as cell viability assays have the potential for developing intestinal organoid models.

Conflict of Interest

The authors declare no conflict of interest.

Acknowledgment

This work is supported by the HIU UNPAD Grant (2022 to SE).

References

1. Edmondson R, Broglie JJ, Adcock AF, Yang L. Three-dimensional cell culture systems and their applications in drug discovery and cell-based biosensors. Assay Drug Dev Technol. 2014;12(4):207–18.
2. Huang SM, Strong JM, Zhang L, Reynolds KS, Nallani S, Temple R, et al. New era in drug interaction evaluation: US Food and Drug Administration update on CYP enzymes, transporters, and the guidance process. J Clin Pharmacol. 2008;48(6):662–70.
3. Duval K, Grover H, Han LH, Mou Y, Pegoraro AF, Fredberg J, et al. Modeling physiological events in 2D vs. 3D cell culture. Physiology (Bethesda). 2017;32(4):266–77.
4. Fowler S, Chen WLK, Duignan DB, Gupta A, Hariparsad N, Kenny JR, et al. Microphysiological systems for ADME-related applications: current status and recommendations for system development and characterization. Lab Chip. 2020;20(3): 446–67.
5. Baudy AR, Otieno MA, Hewitt P, Gan J, Roth A, Keller D, et al. Liver microphysiological systems development guidelines for safety risk assessment in the pharmaceutical industry. Lab Chip. 2020;20(2):215–25.
6. Danielson JJ, Perez N, Romano JD, Coppens I. Modelling *Toxoplasma gondii* infection in a 3D cell culture system in vitro: comparison with infection in 2D cell monolayers. PLoS One. 2018;13(12):e0208558.
7. Derricott H, Luu L, Fong WY, Hartley CS, Johnston LJ, Armstrong SD, et al. Developing a 3D intestinal epithelium model for livestock species. Cell Tissue Res. 2019;375:409–24.
8. Teriyapirom I, Batista-Rocha AS, Koo BK. Genetic engineering in organoids. J Mol Med (Berl). 2021;99(4):555–68.
9. Hofer M, Lutolf MP. Engineering organoids. Nat Rev Mater. 2021;6(5):402–20.
10. Luu L, Johnston LJ, Derricott H, Armstrong SD, Randle N, Hartley CS, et al. An open-format enteroid culture system for interrogation of interactions between *Toxoplasma gondii* and the intestinal epithelium. Front Cell Infect Microbiol. 2019;9:300.
11. Rauth S, Karmakar S, Batra SK, Ponnusamy MP. Recent advances in organoid development and applications in disease modeling. Biochim Biophys Acta Rev Cancer. 2021;1875(2):188527.
12. El-Badri N, Elkhenany H. Toward the nanoengineering of mature, well-patterned and vascularized organoids. Nanomedicine (Lond). 2021;16(15):1255–8.
13. Huang J, Hume AJ, Abo KM, Werder RB, Villacorta-Martin C, Alysandratos KD, et al. SARS-CoV-2 infection of pluripotent stem cell-derived human lung alveolar type 2 cells elicits a rapid epithelial-intrinsic inflammatory response. Cell Stem Cell. 2020;27(6):962–73.e7.
14. Engevik MA, Luck B, Visuthranukul C, Ihekweazu FD, Engevik AC, Shi Z, et al. Human-derived *Bifidobacterium dentium* modulates the mammalian serotonergic system and gut-brain axis. Cell Mol Gastroenterol Hepatol. 2021;11(1):221–48.
15. Wang M, Yu H, Zhang T, Cao L, Du Y, Xie Y, et al. In-depth comparison of matrigel dissolving methods on proteomic profiling of organoids. Mol Cell Proteomics. 2022;21(1):100181.
16. Aisenbrey EA, Murphy WL. Synthetic alternatives to matrigel. Nat Rev Mater. 2020;5(7):539–51.
17. Marapureddy SG, Hivare P, Sharma A, Chakraborty J, Ghosh S, Gupta S,, et al. Rheology and direct write printing of chitosan - graphene oxide nanocomposite hydrogels for differentiation of neuroblastoma cells. Carbohydr Polym. 2021;269:118254.
18. Liu W, Luo H, Wei Q, Liu J, Wu J, Zhang Y, et al. Electrochemically derived nanographene oxide activates endothelial tip cells and promotes angiogenesis by binding endogenous lysophosphatidic acid. Bioact Mater. 2021;9:92–104.
19. Abdelhalim AOE, Meshcheriakov AA, Maistrenko DN, Molchanov OE, Ageev SV, Ivanova DA, et al. Graphene oxide enriched with oxygen-containing groups: on the way to an increase of antioxidant activity and biocompatibility. Colloids Surf B Biointerfaces. 2022;210:112232.
20. Zhang J, Yan L, Wei P, Zhou R, Hua C, Xiao M, et al. PEG-GO@XN nanocomposite suppresses breast cancer metastasis via inhibition of mitochondrial oxidative phosphorylation and blockade of epithelial-to-mesenchymal transition. Eur J Pharmacol.

2021;895:173866.
21. Bayaraa O, Dashnyam K, Singh RK, Mandakhbayar N, Lee JH, Park JT, et al. Nanoceria-GO-intercalated multicellular spheroids revascularize and salvage critical ischemic limbs through anti-apoptotic and pro-angiogenic functions. Biomaterials. 2023;292:121914.
22. Zhou D, Liu H, Han L, Liu D, Liu X, Yan Q, et al. Paintable graphene oxide-hybridized soy protein-based biogels for skin radioprotection. Chem Eng J. 2023;469:143914.
23. Bahtiar A, Hardiati MS, Faizal F, Muthukannan V, Panatarani C, Joni IM. Superhydrophobic Ni-reduced graphene oxide hybrid coatings with quasi-periodic spike structures. Nanomaterials. 2022;12(3):314.
24. Chen Y, Li C, Tsai YH, Tseng SH. Intestinal crypt organoid: isolation of intestinal stem cells, in vitro culture, and optical observation. Methods Mol Biol. 2019;1576:215–28.
25. O'Rourke KP, Ackerman S, Dow LE, Lowe SW. Isolation, culture, and maintenance of mouse intestinal stem cells. Bio Protoc. 2016;6(4):e1733.
26. BE, Lee BJ, Lee KJ, Lee M, Lim YJ, Choi JK, et al. A simple and efficient cryopreservation method for mouse small intestinal and colon organoids for regenerative medicine. Biochem Biophys Res Commun. 2022;595:14–21.
27. Bera M, Chandravati, Gupta P, Maji PK. Facile one-pot synthesis of graphene oxide by sonication assisted mechanochemical approach and its surface chemistry. J Nanosci Nanotechnol. 2018;18(2):902–12.
28. Pérez-Molina Á, Morales-Torres S, Maldonado-Hódar FJ, Pastrana-Martínez LM. Functionalized graphene derivatives and TiO2 for high visible light photodegradation of azo dyes. Nanomaterials (Basel). 2020; 10(6):1106.
29. Prodan D, Moldovan M, Furtos G, Saroşi C, Filip M, Perhaiţa I, et al. Synthesis and characterization of some graphene oxide powders used as additives in hydraulic mortars. Appl Sci. 2021;11(23):11330.
30. Wang N, Zhang H, Zhang BQ, Liu W, Zhang Z, Qiao M, et al. Adenovirus-mediated efficient gene transfer into cultured three-dimensional organoids. PLoS One. 2014;9(4):e93608.
31. Han SH, Shim S, Kim MJ, Shin HY, Jang WS, Lee SJ, et al. Long-term culture-induced phenotypic difference and efficient cryopreservation of small Intestinal organoids by treatment timing of Rho kinase inhibitor. World J Gastroenterol. 2017;23(6):964–75.
32. Sumigray KD, Terwilliger M, Lechler T. Morphogenesis and compartmentalization of the intestinal crypt. Dev Cell. 2018;45(2):183–97.e5.
33. Rahmawati L, Puspitasari IM. Teknik pembuatan kultur sel primer, immortal cell line dan stem cell. Farmaka. 2016;14(2):195–206.
34. Barker N, van Es JH, Kuipers J, Kujala P, van den Born M, Cozijnsen M, et al. Identification of stem cells in small intestine and colon by marker gene *Lgr5*. Nature. 2007;449:1003–7.
35. Joshi CJ, Ke W, Drangowska-Way A, O'Rourke EJ, Lewis NE. What are housekeeping genes? PLoS Comput Biol. 2022;18(7):e1010295.
36. Rácz GA, Nagy N, Tóvári J, Apáti Á, Vértessy BG. Identification of new reference genes with stable expression patterns for gene expression studies using human cancer and normal cell lines. Sci Rep. 2021;11(1):19459.
37. Cherubini A, Rusconi F, Lazzari L. Identification of the best housekeeping gene for RT-qPCR analysis of human pancreatic organoids. PLoS One. 2021;16(12):e0260902.
38. Dieterich W, Neurath MF, Zopf Y. Intestinal ex vivo organoid culture reveals altered programmed crypt stem cells in patients with celiac disease. Nat Res. 2020;10(1):3535.
39. Wang X, Yamamoto Y, Wilson LH, Zhang T, Howitt BE, Farrow MA, et al. Cloning and variation of ground state intestinal stem cells. Nature. 2015;522(7555):173–8.
40. Bonis V, Rossell C, Gehart H. The intestinal epithelium – fluid fate and rigid structure from crypt bottom to villus tip. Front Cell Dev Biol. 2021;9:661931.
41. Snippert HJ, van der Flier LG, Sato T, van Es JH, van den Born M, Kroon-Veenboer C, et al. Intestinal crypt homeostasis results from neutral competition between symmetrically dividing Lgr5 stem cells. Cell. 2010;143(1):134–44.
42. Dame MK, Attili D, McClintock SD, Dedhia PH, Ouillette P, Hardt O, et al. Identification, isolation and characterization of human Lgr5-positive colon adenoma cells. Development.

2018;145(6):dev153049.
43. Pracht K, Wittner J, Kagerer F, Jäck HM, Schuh W. The intestine: a highly dynamic microenvironment for IgA plasma cells. Front Immunol. 2023;14:1114348.
44. Yao X, Zhan L, Yan Z, Li J, Kong L, Wang X, et al. Non-electric bioelectrical analog strategy by a biophysical-driven nano-micro spatial anisotropic scaffold for regulating stem cell niche and tissue regeneration in a neuronal therapy. Bioact Mater. 2023;20:319–38.
45. Biru EI, Necolau MI, Zainea A, Iovu H. Graphene oxide-protein-based scaffolds for tissue engineering: recent advances and applications. Polymers (Basel). 2022;14(5):1032.
46. Lu P, Zehtab Yazdi A, Han XX, Al Husaini K, Haime J, Waye N, et al. Mechanistic insights into the cytotoxicity of graphene oxide derivatives in mammalian cells. Chem Res Toxicol. 2020;33(9):2247–60.
47. Zhao H, Gu B, Yang P, Yi J, Lv X. Antibacterial properties and mechanism of graphene oxide with different C/O ratio. J Phys Conf Ser. 2023;2468:012002.
48. Asadi Shahi S, Roudbar Mohammadi S, Roudbary M, Delavari H. A new formulation of graphene oxide/fluconazole compound as a promising agent against *Candida albicans*. Prog Biomater. 2019;8(1):43–50.
49. Sekuła-Stryjewska M, Noga S, Dźwigońska M, Adamczyk E, Karnas E, Jagiełło J, et al. Graphene-based materials enhance cardiomyogenic and angiogenic differentiation capacity of human mesenchymal stem cells in vitro – focus on cardiac tissue regeneration. Mater Sci Eng C Mater Biol Appl. 2021;119:111614.